Splashing on elastic membranes: The importance of early-time dynamics

Rachel E. Pepper,[1] Laurent Courbin,[2] and Howard A. Stone[2]
[1]*Department of Physics, Harvard University, Cambridge, Massachusetts 01238, USA*
[2]*School of Engineering and Applied Sciences, Harvard University, Cambridge, Massachusetts 02138, USA*

We study systematically the effect of substrate compliance on the threshold for splashing of a liquid drop using an elastic membrane under variable tension. We find that the splashing behavior is strongly affected by the tension in the membrane and splashing can be suppressed by reducing this tension. The deflection of the membrane upon droplet impact is measured using a laser sheet, and the results allow us to estimate the energy absorbed by the film upon drop impact. Measurements of the velocity and acceleration of the spreading drop after impact indicate that the splashing behavior is set at very early times after, or possibly just before, impact, far before the actual splash occurs. We also provide a model for the tension dependence of the splashing threshold based on the pressure in the drop upon impact that takes into account the interplay between membrane tension and drop parameters. © 2008 American Institute of Physics. [DOI: 10.1063/1.2969755]

I. INTRODUCTION

The impact of a liquid droplet on a solid substrate and the subsequent splash—defined as the detachment of small satellite droplets from the spreading drop—is a common everyday phenomenon. Despite splashing's ubiquity, both in our personal experience, and in such diverse applications as ink-jet printing,[1,2] fuel combustion,[3] industrial spray coating,[4] and pesticide delivery,[5,6] the mechanism of such splashes is not yet fully understood. For some applications, such as fuel combustion, splashing is beneficial, while for others, such as pesticide delivery, splashing should be minimized. For these reasons, it is important to understand the splash mechanism, as well as which parameters can be used to effectively control splashing behavior. For a recent review of splashing phenomena, see Ref. 7.

There are three components in such drop-surface impacts: the liquid droplet, the surrounding gas, and the solid substrate. The relevant parameters of the liquid can be characterized using two dimensionless groups, $\mathrm{Re}=2\rho R_0 V_0/\mu$ and $\mathrm{We}=2\rho R_0 V_0^2/\gamma$, where ρ, μ, and γ are the density, viscosity, and surface tension of the liquid, respectively, and R_0 and V_0 are the radius and impact velocity of the drop. These dimensionless groups are combined in an oft-cited empirical relation for the splashing threshold, which involves liquid drop parameters only and does not include parameters of the substrate or gas: $\mathrm{We}^{1/2}\,\mathrm{Re}^{1/4}=K$; based on the data from several sources, splashing occurs for $K \geq K_d \simeq 50$.[8] A scaling argument for this correlation is given by Roisman *et al.*,[9] who balanced inertial and capillary effects for impacts on dry smooth substrates. A rationalization of the functional form is also available for splashing for a train of droplets[10] and on a thin liquid film.[11]

Recently, it has been shown by Xu *et al.*[12] that the gas surrounding the impact plays an important role in splashing: the splash can be suppressed completely by reducing the pressure of the surrounding gas. We note that the surrounding gas pressure and composition have also been shown to be important in binary droplet collisions, where the assumption was made that the gas affected the dynamics leading to contact.[13]

The characteristics of the solid substrate, for example, roughness and surface chemistry, also affect splashing behavior. Based on the roughness of the substrate, Stow and Hadfield[14] proposed an empirical splashing threshold of the form $\mathrm{We}^{1/2}\,\mathrm{Re}^{1/4}=\xi(R_a)$, where R_a is the roughness of the substrate, defined as the mean absolute deviation about the mean surface level. Additional studies of roughness are reported in Refs. 15 and 16. More recently, Courbin *et al.*[17] indicated qualitatively the effect of rough and microtextured surfaces on the splashing threshold, which has subsequently been studied more systematically.[18]

A second feature of the surface that plays a role in the physics of splashing is wettability, which is determined both by surface roughness and surface chemistry. For example, Duez *et al.*[19] investigated the impact of a solid sphere with a liquid-gas interface. They found that the critical velocity for air entrainment was dependent on the equilibrium contact angle and that superhydrophobic spheres create large splashes for any impact velocity. A hint that surface chemistry is also important in impacts of liquid drops on solid substrates comes from data that show different values for the splash threshold on substrates of the same roughness but different contact angles.[14,16]

The role of the compliance of soft substrates on drop splashing is important to understand since it is involved in many common applications, such as pesticide spray on leaves and spray cooling of flexible surfaces. However, to our knowledge, the sole report of splashing on compliant substrates was given by Field *et al.*,[20] who focused only on erosion damage for impacts at speeds far above the splashing threshold (>100 m/s).

In this paper, we report a comprehensive study of the effect of substrate compliance on the splash threshold using an elastic membrane under variable tension. We find that decreasing the tension in the elastic sheet increases the
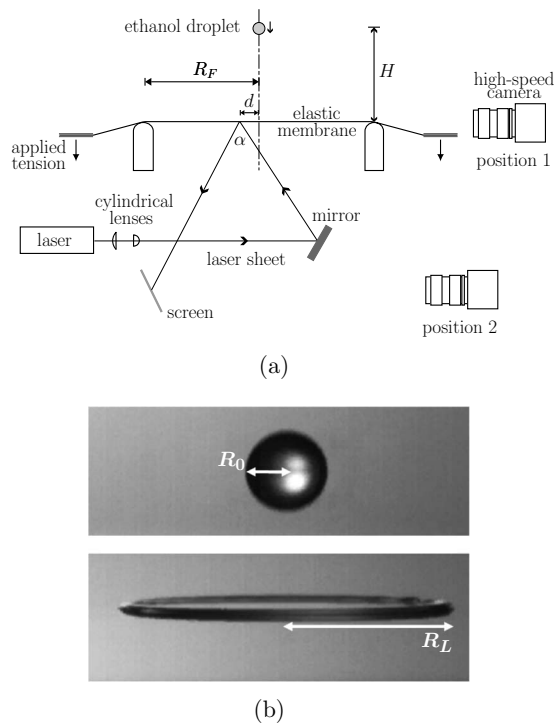
FIG. 1. (a) Schematic of the experimental setup. For splash threshold measurements, a high-speed camera was placed in position 1, and the laser was off. For membrane deflection measurements, a high-speed camera was used either in position 1 or position 2 but never in both simultaneously. The scale is compressed in the vertical direction; in the actual experiments $\alpha \simeq 20°$. (b) Typical images taken from high-speed movies before (upper image) and after (lower image) impact for the same millimeter-size drop (camera in position 1).

threshold velocity for splashing. This tuning with tension is first examined using energy balances. We then investigate the dynamics of the spreading lamella, which suggests that splashing behavior is set at early times after impact. Finally, we present a model for the splashing threshold as a function of the tension in the membrane, which allows us to rationalize the experimental trends for splashing on elastic substrates.

II. EXPERIMENTAL METHODS

A. Drop impact setup

A schematic of the experimental setup is shown in Fig. 1(a). An elastic membrane was clamped (taking care not to introduce any initial pretension) between two Plexiglas rings (inner diameter of 19.05 ± 0.01 cm and outer diameter of 26.67 ± 0.01 cm) and placed onto a lubricated cylindrical frame (radius $R_F = 5.24 \pm 0.01$ cm). This setup allows for application of uniform tension to the membrane without wrinkling (see Ref. 21 for additional information on a similar setup used in a previous study). This tension can be tuned by placing additional brass rings on the Plexiglas clamping ring, which allowed us to apply tensions T between 17 ± 2 and 55 ± 2 N/m.

The elastic membrane used in these experiments was Saran Wrap (Johnson), which is a stretchable polymer film of low Young's modulus with thickness of approximately

10 μm and density of approximately 1.7 g/cm^3.[21] To create a solid surface of effectively infinite tension, but with the same wetting and roughness properties as Saran Wrap, the membrane was placed over a smooth solid surface, while taking care that no bubbles were present between the solid and the Saran Wrap.

Millimeter-radius ethanol drops (viscosity $\mu = 1.2 \times 10^{-3}$ Pa s, density $\rho = 789$ kg/m^3, and surface tension $\gamma = 0.02$ N/m) were released from rest above the center of the membrane, and the impacts were observed using a Phantom high-speed video camera recording at a rate between 13 000 and 100 000 frames/s. Drops of reproducible size were generated using a syringe pump to slowly create pendant drops, which subsequently fell under their own weight. The drop radii were adjusted between 1.01 ± 0.02 mm and 1.63 ± 0.02 mm using needles of different inner diameters. For larger drops, oscillations of the droplet shape during free fall become noticeable. Only experiments for which the drops were approximately spherical on impact (eccentricity < 0.3) were analyzed. By adjusting the height of release H, we changed the impact speed V_0 in the range of 1–3.5 m/s. We used custom-written MATLAB image-analysis software to determine the impact velocity, initial droplet radius, and the evolution in time of the radius R_L of the expanding liquid sheet or lamella [see Fig. 1(b)]. When determining the splashing threshold, a splash was defined as any impact in which secondary droplets were emitted from the periphery of the expanding lamella. Over 600 individual experiments were analyzed to determine splashing thresholds.

B. Membrane deflection setup

The deflection of the center point of the membrane upon impact was measured using reflection of a laser sheet off of the bottom surface of the membrane [see Fig. 1(a) for a schematic]. The beam of an unpolarized helium-neon laser (17 mW, 633 nm) was passed through two half cylindrical lenses to create a laser sheet of uniform width ($\simeq 5$ cm) which was then reflected onto the bottom surface of the elastic membrane. The membrane functioned as a semitransparent mirror: most of the laser sheet passed through the membrane, but some was reflected to a screen below, where the resulting laser line was recorded using our high-speed imaging system. Since the position of this laser line is highly dependent on the angle at which the laser meets the membrane, small changes in the membrane position and thus angle result in large changes in the recorded position of the laser line (see Fig. 2).

The setup for deflection measurements was calibrated by dropping stainless steel spheres with radii between 0.5 and 1.75 mm onto the membrane using a custom-made electromagnet (as described in Ref. 21). In contrast to liquid drops, stainless steel spheres do not deform upon impact, and the evolution in time of the deflection of the center of the membrane $\delta(t)$ can be measured by tracking the position of the top of the sphere (see Fig. 2). We constructed a calibration curve by recording the maximum laser line deflection (with a camera in position 2) for several sphere radius/height of re-
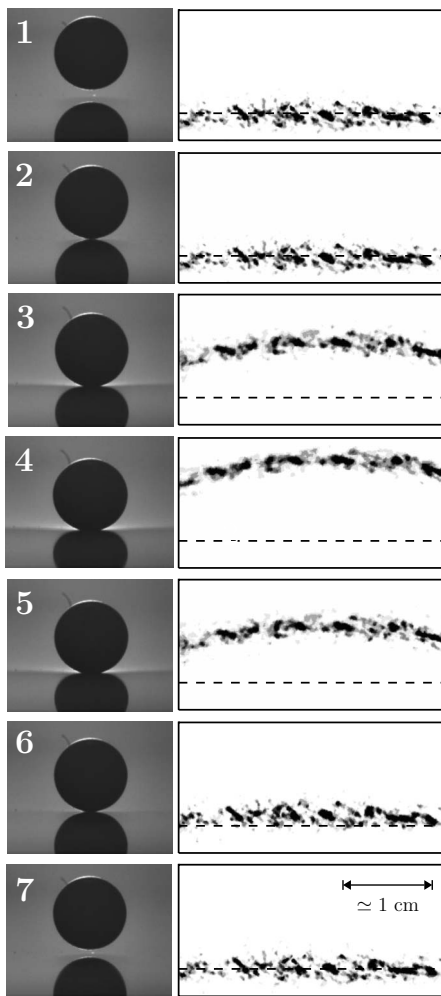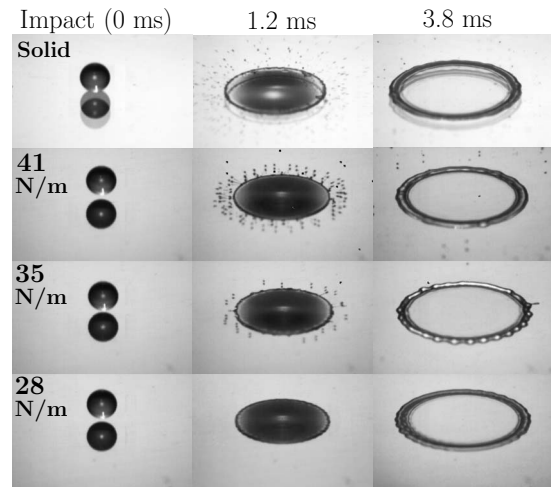
FIG. 2. Example images taken from high-speed movies during the impact of a 1.25 mm radius stainless steel sphere with $V_0 = 0.28 \pm 0.01$ m/s. The right side image is of the screen indicated in Fig. 1(a) (camera in position 2); the dashed line indicates the initial position of the laser line. To the left are the corresponding photos of the stainless steel sphere at the same times (camera in position 1). The reflection of the sphere can be seen in the substrate. Impact occurs in frame 2, and the frames are taken at 0.75 ms intervals. The maximum deflection of the membrane for this impact (which occurs in frame 4) is 0.29 ± 0.02 mm. Screen images and sphere images were matched from separate impacts with a matching error of 0.04 ms. $T = 28 \pm 2$ N/m.

FIG. 3. (a) High-speed images of drop impact ($R_0 = 1.01 \pm 0.02$ mm, $V_0 = 2.5 \pm 0.1$ m/s) on membranes of varying tension. Each row shows the drop at three times: just before impact, 1.2 ms, and 3.8 ms after impact. The top row is for impact on a solid (plastic Petri dish). (b) Threshold velocity for splashing vs membrane tension for drops with $R_0 = 1.01 \pm 0.02$ mm. Error bars show the transition regime—above the top error bar, splashing always occurs; below the bottom error bar, splashing never occurs. The midpoint is defined as the threshold velocity. The solid line at $V_T = 2.2$ m/s is the splashing threshold on a solid surface with the same roughness and wettability as the membrane; the dashed lines represent the error in this measurement. Inset: the threshold velocity for splashing vs membrane tension for three different drop sizes: (●) $R_0 = 1.01 \pm 0.02$ mm, (□) $R_0 = 1.12 \pm 0.02$ mm, and (∗) $R_0 = 1.63 \pm 0.02$ mm. Solid and dashed lines are for impact on a solid for droplets of $R_0 = 1.01$ mm and $R_0 = 1.12$ mm, respectively. Error bars have been omitted for clarity.

lease pairs whose actual maximal deflection δ_{max} we had already measured (with a camera in position 1). We found a linear relationship between the maximum laser line deflection and the maximum membrane deflection (data not shown here). This calibration is clearly sensitive to the distance d between the laser sheet and the point of impact [see Fig. 1(a)], which was fixed at $d = 1$ cm.
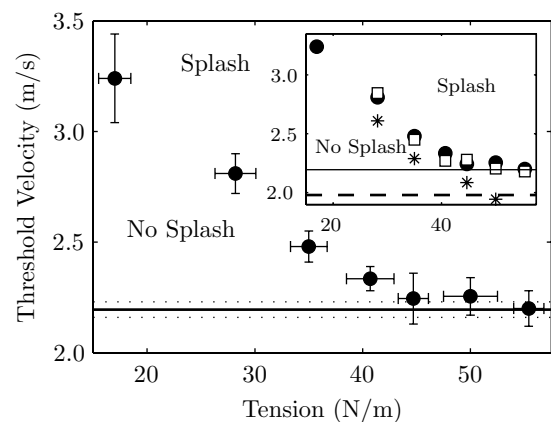
III. RESULTS AND DISCUSSION

A. The influence of membrane tension

High-speed images illustrating the influence of membrane tension on the splash threshold are shown in Fig. 3(a). We observe that splashing behavior is strongly affected by the tension in the membrane and that splashing can be suppressed by reducing this tension. We report the threshold impact velocity V_T above which splashing occurs as a func-

tion of the tension in the membrane for three different drop radii in Fig. 3(b). The threshold velocity is highest for the lowest membrane tension; as the tension in the membrane increases, the threshold velocity decreases, approaching the threshold velocity for impact on a solid substrate.

We observe a variety of phenomena during the impact of a drop with the membrane. These phenomena are organized in a time line of dynamical events during a sample impact in Fig. 4. The time sequence obtained for particular impact parameters (see the caption of Fig. 4) is representative, within the range of our experiments, of the ordering of events and the order of magnitude of the times involved. At impact, the membrane deflects downward (the dashed line in Fig. 4
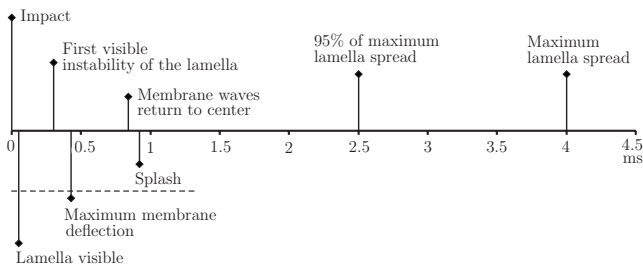
FIG. 4. Time line for a typical splash on a flexible membrane. The dashed line represents the interval over which the membrane is deflected downward after impact. The impact parameters are $R_0 = 1.12 \pm 0.02$ mm, $V_0 = 2.3 \pm 0.1$ m/s, and $T = 41 \pm 2$ N/m.
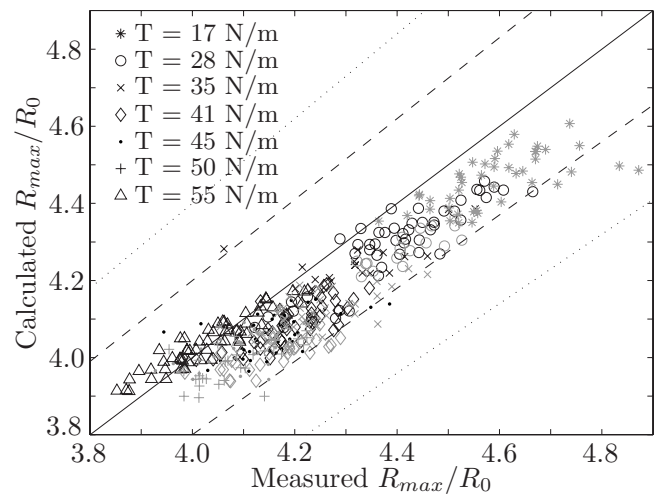

FIG. 5. Comparison of the calculated maximum spread using Eq. (2) with the measured maximum spread for data taken for impact on membranes of different tensions. Gray symbols, $R_0 = 1.01 \pm 0.02$ mm. Black symbols, $R_0 = 1.12 \pm 0.02$ mm. The solid line with slope 1 represents an exact match between experiments (x-axis) and theoretical predictions (y-axis); the dashed line represents a 5% variation from the solid line, and the dotted line a 10% variation.

shows the interval over which the membrane is deflected downward), with the maximum deflection occurring at $\simeq 0.4$ ms after impact. Simultaneously, a lamella emerges from under the drop (first visible at $\simeq 0.05$ ms) and becomes visibly ruffled (at $\simeq 0.3$ ms). The lamella continues to spread, with the splash occurring at $\simeq 0.8$ ms. After droplets are emitted, the lamella spreads further, reaching its maximum radius at $\simeq 4$ ms. Examining the time line in Fig. 4, we see a rich variety of behaviors occuring at early times (<1 ms), while later we observe only spreading of the liquid sheet.

With this difference in time scales in mind, we next examine two different energy balances: one at late times and one at early times. The late-time energy balance compares energies at the time of drop impact and at the time of maximum lamella spread (the first and last points in the time line in Fig. 4), while the early-time energy balance examines energies at the time of drop impact and at the time of maximum membrane deflection (the first and fourth points in the time line in Fig. 4). As shown below, we find that the change in splashing threshold with membrane tension cannot be explained by considering the late-time energy balance, but that the early-time energy balance reveals a possible energy threshold for splashing.

B. Late-time energy balance

In the literature, a late-time energy balance is often used to calculate the maximum lamella spread, $R_{\max}/R_0$, where $R_{\max}$ is the maximum radius of the lamella.[8,22–27] An overview of several approaches is provided in Ref. 26. In general, the initial kinetic and surface energies of the spherical drop at the moment of impact are balanced with the surface energy of the flattened drop at the moment of maximum lamella spread (when kinetic energy is assumed negligible), and the energy dissipated while spreading,

$$E_k + E_s = E_s' + E_d, \tag{1}$$

where E_k and E_s are the kinetic and surface energies of the drop at impact, E_s' is the surface energy of the drop at the time of maximum spread, and E_d is the energy dissipated during the spread. The left-hand side of Eq. (1) can be derived straightforwardly ($\frac{2}{3}\pi R_0^3 \rho V_0^2 + 4\pi\gamma R_0^2$, where ρ and γ are the density and surface tension of the liquid). To estimate the right-hand side, we use the result of Mao et al.,[24] as they

find that their semiemperical maximum spread model fits 90% of the experimental data (both from their experiments and those of others) within 10%,

$$\left[\frac{1}{4}(1 - \cos\theta) + 0.2\frac{\text{We}^{0.83}}{\text{Re}^{0.33}} \right]\left(\frac{R_{\max}}{R_0} \right)^3 - \left(\frac{\text{We}}{12} + 1 \right)$$

$$\times \left(\frac{R_{\max}}{R_0} \right) + \frac{2}{3} = 0, \tag{2}$$

where θ is the static contact angle between the substrate and the liquid (in our case $\theta = 40° \pm 5°$). The prefactor and exponents in the We/Re term are fitted parameters; we use the same parameters as Mao et al.[24] Figure 5 shows the comparison between Eq. (2) and our experimental values for $R_{\max}/R_0$; note that Eq. (2) was calculated for impacts on a solid substrate and does not include any energy lost to the membrane. Nevertheless, a strong correlation is found: six different membrane tensions and two droplet sizes all collapse onto a single curve which is within less than 10% of the model of Mao et al.

The collapse of the data from all of the membrane tensions onto one curve shows that membrane effects are negligible at late times, and thus a late-time energy balance cannot explain the tuning of the splash with tension that we observe (Fig. 3). It is reasonable that such a late-time approach does not provide insight on the splashing threshold since the splash occurs much earlier than does the maximum lamella radius (see Fig. 4).

C. Early-time energy balance

We next consider an early-time energy balance. We observe that, at times shortly after impact, the liquid velocity is of the same order as the impact velocity and surface energy is negligible compared with kinetic energy. For instance, at the splash threshold for drops of radius

TABLE I. Maximum deflection of the membrane measured at the threshold velocity for splashing. $R_0 = 1.12 \pm 0.02$ mm.

Tension (N/m)	V_0 (m/s)	δ_{max} (mm)
28 ± 2	2.8 ± 0.1	0.59 ± 0.05 [a]
35 ± 2	2.4 ± 0.1	0.33 ± 0.05
41 ± 2	2.3 ± 0.1	0.22 ± 0.02
45 ± 1	2.3 ± 0.1	0.17 ± 0.03
50 ± 3	2.3 ± 0.1	0.13 ± 0.02
55 ± 2	2.2 ± 0.1	0.06 ± 0.03

[a]Due to experimental restrictions, this value was extrapolated from maximum deflection values for lower impact velocities.

$R_0 = 1.12 \pm 0.02$ mm on a membrane with a tension $T = 55 \pm 2$ N/m, the Weber number is We$= 420 \pm 20$, the kinetic energy is approximately $E_k \approx 11$ μJ, and the surface energy is approximately $E_s \approx 0.3$ μJ. We also neglect energy lost through viscous dissipation in the fluid and vibrational energy in the membrane. Therefore, we compare the kinetic energy of the drop at impact E_k with the elastic energy stored in the membrane at the time of maximum deflection E_m' and the kinetic energy remaining in the drop E_k',

$$\frac{2}{3}\pi R_0^3 \rho V_0^2 = E_m' + E_k'. \tag{3}$$

The prime indicates values taken at the time of maximum membrane deflection. We examine this energy balance at the splashing threshold determined in Fig. 3, i.e., $V_0 = V_T$.

In order to calculate E_m', the maximum membrane displacement δ_{max} was measured for impacts at V_T using our setup for deflection measurements (see Table I). The elastic energy stored in an elastic sheet is $E_m = T/2 \int dS (\nabla \boldsymbol{v})^2$, where the integration is over the surface of the membrane, and $\boldsymbol{v}(\boldsymbol{r})$ is the displacement of the membrane from its equilibrium position.[28] Using the shape of a circular membrane with displacement δ_{max} at the center yields the estimate

$$E_m' = \frac{\pi}{\ln\left(\frac{\ell}{\sqrt{\delta_{max} R_0}}\right)} T \ell^2 \left(\frac{\delta_{max}}{\ell}\right)^2, \tag{4}$$

where ℓ is the typical length over which the membrane is deformed, R_0 is the radius of the droplet, and T is the tension in the membrane.[21] The value of ℓ was calculated using transverse membrane speeds c_t measured with our laser setup, and the measured time t' of maximum membrane deflection; $\ell = t' c_t$.[21] The relevant energies, E_m', E_k, and $E_k' = E_k - E_m'$ are plotted in Fig. 6 for the deflection data in Table I. As depicted in this figure, E_k', the estimate of the kinetic energy that remains in the drop following impact, is approximately constant at the splashing threshold. This experimental result indicates that there may be a critical (radius-dependent) kinetic energy after impact (later converted to spreading and splashing) necessary for a splash. We would expect the critical kinetic energy after impact to have the same value as the kinetic energy splash threshold on a solid, while we can see in Fig. 6 that the value for the threshold on a solid (horizontal solid line) is slightly smaller. This difference could potentially be corrected by accounting for
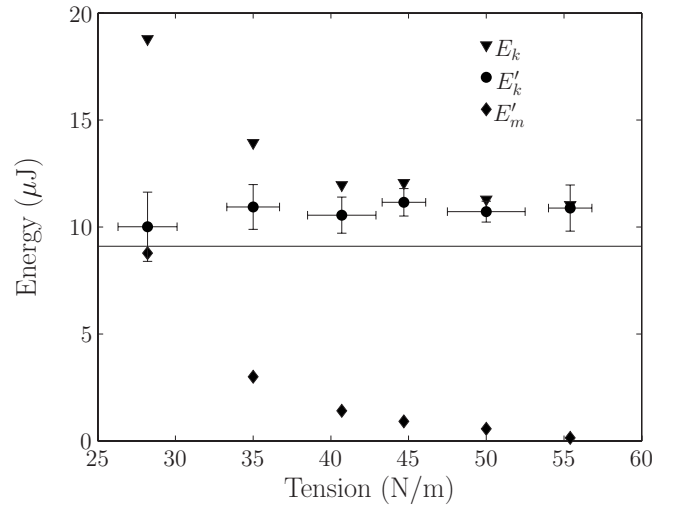

FIG. 6. Comparison of energies. The kinetic energy at impact E_k was calculated from the threshold velocity data used in Fig. 3. The solid line represents the kinetic energy at the threshold for splashing on a solid substrate. The energy in the membrane at the time of maximum membrane deflection E_m' was calculated from Eq. (4) using the values in Table I. Note that these deflection values are taken for impacts at the threshold velocity for splash. The kinetic energy in the liquid at the time of maximum membrane deflection E_k' was calculated from $E_k' = E_k - E_m'$. Some error bars have been omitted for clarity of viewing. The remaining error bars are of approximately the same magnitude as those omitted. $R_0 = 1.12 \pm 0.02$ mm.

the energy lost to viscous dissipation when calculating E_k'. If such a kinetic energy threshold exists, it is reasonable to assume that it depends on drop and surface parameters not explored in the present study and further points toward the importance of the initial condition data in understanding splashing.

It is intuitive that an elastic membrane increases the threshold for splashing by converting some of the kinetic energy at impact into stored elastic energy. A more flexible membrane stores more energy and suppresses splashing more effectively. However, part of this stored elastic energy is again converted to kinetic energy as the membrane returns toward the flat state, and some of this kinetic energy may be returned to the liquid. This leaves the question of timing: at what time after impact is the kinetic energy in the droplet a critical parameter? Our data do not have the precision to answer this question, although the time of maximum membrane deflection was from 0.4 ± 0.1 to 0.5 ± 0.1 ms, depending on the tension in the membrane. It is also possible that the membrane affects the splash through a completely different mechanism, and that the apparent kinetic energy threshold is a coincidence or a consequence of this unseen mechanism. For instance, it is possible that a flexible membrane increases the splash threshold by reducing the pressure of the air in between the drop and the surface in the instants before impact. Unlike a solid, the membrane would respond to high pressure under the drop by flexing, limiting this maximum pressure. Such a mechanism, which involves a reduction in air pressure, might be consistent with the results reported by Xu et al.[12] The change in splash threshold could also be due to the change in the relative impact velocities due to the
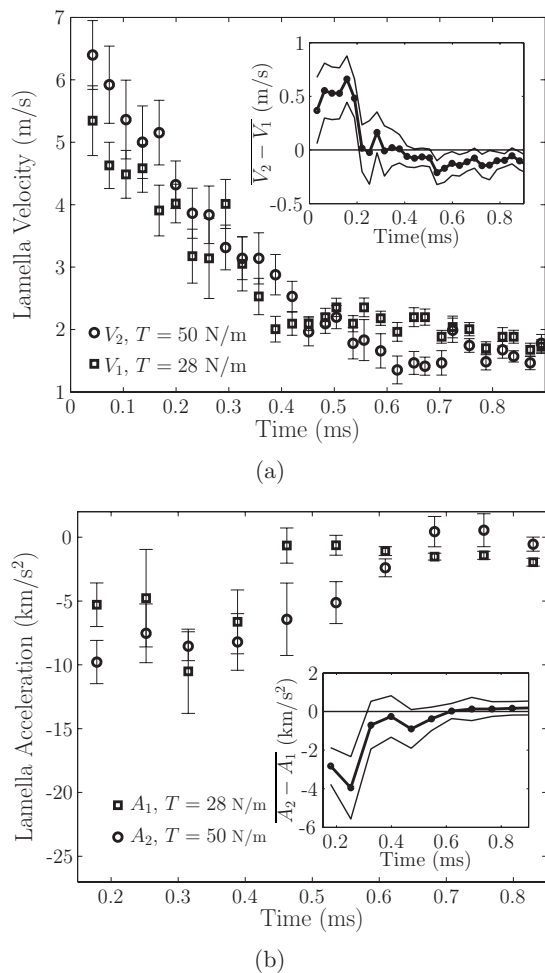
FIG. 7. (a) The main panel shows the velocity of the lamella (dR_L/dt) as a function of time after impact for two representative impacts at different tensions ($R_0 = 1.01 \pm 0.02$ mm and $V_0 = 2.6 \pm 0.1$ m/s). The inset plot shows the difference between the lamella velocity for impacts on membranes of $T = 50 \pm 3$ N/m and of $T = 28 \pm 2$ N/m averaged over 15 pairs of impacts (each with identical parameters except T) at 5 different impact speeds ($V_0 = 2.0 - 2.8 \pm 0.1$ m/s). In four of these pairs, splashing was observed for the impact on the membrane of $T = 50 \pm 3$ N/m. Thinner lines represent error bars. (b) Acceleration of the lamella (d^2R_L/dt^2) as a function of time. The main panel and inset correspond to the plots in (a) with one further derivative of R_L. The R_L vs time data were smoothed with a window size of three time points for velocity and seven time points for acceleration in order to get smooth velocity and acceleration plots. The videos used to generate R_L vs time data were filmed at 95 238 frames/s; therefore, one time point is 10.5 μs.

motion of the membrane. We discuss this possible mechanism in Sec. III E by considering the impulse at impact.

D. Lamella dynamics

Further insight into the splashing mechanism can be gained by examining the dynamics of the spreading lamella using high-speed imaging. When drops of the same size and impact velocity are compared, we find that, at early times after impact, the velocity of the expanding liquid sheet (dR_L/dt) is larger for higher tensions [see Fig. 7(a)]. Similarly, shortly after impact, the deceleration of the lamella (d^2R_L/dt^2) is larger for larger tensions [see Fig. 7(b)]. While these are mostly within the range of error for individual pairs

of impacts (as in the main panels of Fig. 7), the differences become clear when averaged over multiple pairs of impacts (see inset plots of Fig. 7). It is likely that differences in lamella spreading velocity and acceleration are responsible for the different splash thresholds observed for different membrane tensions. The velocity and acceleration differences among different tensions are significant only in the first 0.4 ± 0.1 ms after impact. Comparing this time with the time line in Fig. 4, we can see that this is far before the typical time of splashing (defined as the pinching off of secondary droplets) which occurs at $\simeq 0.8$ ms but near the time at which the first instabilities are visible in the lamella at $\simeq 0.3$ ms.

If we assume that, for the given liquid properties, splashing is controlled by the velocity and acceleration of the lamella, our results suggest that the splashing instability is formed at very early times after impact (or even immediately before impact[29]), far before the actual splash occurs. This argument is consistent with our results on the early-time energy balance, as a possible kinetic energy threshold was seen at $\simeq 0.4$ ms. It is also consistent with the argument that the splashing mechanism is derived from a Rayleigh–Taylor (RT) type instability.[30] Allen,[31] who first proposed the RT instability as a mechanism for splashing, noted that the necessary lamella deceleration was surprisingly high, of the order of $700g$ for impacts such as those in our experiments. Using the analysis of impact in Ref. 30 gives a similarly high acceleration: $R_L(t) \sim \sqrt{2R_0V_0t}$, which is estimated from the base of a spherical drop, with volume of approximately $2\ell^2 R_0$, where $\ell = V_0t$, being displaced into a radial film of radius R_L and thickness comparable to ℓ. This time dependence yields $d^2R_L/dt^2 \sim -\sqrt{R_0V_0}/(2t)^{3/2}$. Using typical values, $V_0 = 2$ m/s and $R_0 = 1$ mm, and evaluating at our first acceleration time point, $t = 0.115$ ms, we find that $d^2R_L/dt^2 \simeq -1300g$, while our experimental results give $d^2R_L/dt^2 \simeq -1000g$ [see Fig. 7(b)]. Our experimentally measured accelerations are of the same order of magnitude as those predicted by Allen.[31] We are not aware of any previous direct measurement of lamella deceleration.

Xu $et\ al.$[12] proposed a different splashing mechanism that is independent of time. It is difficult to compare our results with their theory as our experiments, performed at atmospheric pressure, are in a different pressure regime. It seems likely, however, that the effects of air compression that are used in their calculations would only be present at very early times, in the instants just before and after impact.[12]

E. Model for the tension dependence of the threshold velocity

As previously shown, our experimental findings reveal the importance of early-time dynamics. We therefore rationalize our data using an early-time model for the threshold velocity as a function of tension, derived from the impulse at impact. The following model is approximate, is essentially one dimensional, and attempts to characterize the influence of the elastic substrate on the initial motion of the liquid. Motivation for this characterization was inspired by Antkow-

iak et al.,[32] who used this impulse pressure approach to explain jetting after impact of a test tube filled with a wetting liquid. For times shortly after contact with the substrate, when the viscous boundary layer is small compared to the drop dimensions, but longer than the compressibility time scale ($\simeq 10^{-6}$ s for experiments such as ours), the Navier–Stokes equation reduces to

$$\rho \frac{\partial \mathbf{u}}{\partial t} = -\nabla p, \tag{5}$$

where $\mathbf{u}$ is the fluid velocity and p is the pressure in the fluid. Following Ref. 32, we integrate both sides with respect to time to obtain $\rho[\mathbf{u}(t) - \mathbf{u}(0)] = -\nabla \int_0^t p \, d\tau$. For the bottom edge of the drop, at some time t shortly after impact, $\mathbf{u}(t) = \mathbf{0}$, $\mathbf{u}(0) = -V_0 \hat{\mathbf{y}}$, giving $\rho V_0 \simeq \partial p / \partial n t$, where we have approximated the integral and used the fact that the velocity at the bottom of the drop points in the outward normal direction to the drop surface, $\hat{\mathbf{n}}$ ($\hat{\mathbf{y}}$ is the vertical direction). Using r as the typical length scale along the flow gives an estimate for the pressure in the fluid $p \simeq \rho V_0 r / t$. As previously mentioned, for drop impacts, $r = R_L(t) \sim \sqrt{2R_0 V_0 t}$,[30] which yields

$$p \simeq \rho V_0^{3/2} R_0^{1/2} t^{-1/2}. \tag{6}$$

We note that the same equation can be found from scaling arguments: from Eq. (5) we expect $p = \mathcal{O}(\rho u r / t)$, which yields Eq. (6) when we substitute $r = R_L$ and $u = V_0$. In this equation, the time dependence is simply indicative of the rate at which pressure changes will occur; nevertheless, we realize that the actual flow response is likely more complicated.

For an elementary model of the reduction in pressure in the liquid due to the flexibility of the membrane, we estimate $\mathbf{u}(t) = -\dot{\delta} \hat{\mathbf{y}}$, where $\delta(t)$ is, as before, the downward deflection of the center of the membrane as a function of time after impact. This substitution gives a modification of Eq. (6) $p \simeq \rho(V_0 - \dot{\delta}) R_L / t$. We next equate the pressure in the fluid p to the elastic stress due to the membrane σ in order to obtain an estimate for $\delta(t)$. An estimate for σ due to the deflection at distance δ of a membrane under a tension T is $\sigma = (T\delta)/(\pi R_L^2)$. Equating $p = \sigma$, we find $\delta \simeq \pi \rho R_L^3 (V_0 - \dot{\delta})/(Tt) \simeq \pi \rho R_0^{3/2} V_0^{3/2} t^{1/2} (V_0 - \dot{\delta})/T$. Since at time scales of milliseconds we expect $\dot{\delta} \ll V_0$, we finally approximate

$$\delta \simeq \pi \rho R_0^{3/2} V_0^{5/2} t^{1/2} / T. \tag{7}$$

We will next use this result for the membrane deflection to estimate the splashing threshold V_T as a function of the tension T. Previous scaling arguments for the splashing threshold[9] utilized the speed of liquid in the lamella ($\approx V_0$) at a time comparable to the spread of the lamella ($\approx 2R_0/V_0$). Here, without a detailed theory, we take into account the change in the speed of the liquid due to the deflection of the flexible membrane by estimating the lamella fluid velocity as $V_0 - \dot{\delta}$. We assume that the splashing threshold is governed by $V_T - \dot{\delta}^* = V_{TS}$, where V_{TS} is the splash threshold on a solid, i.e., when $\dot{\delta} = 0$, and $\dot{\delta}^*$ is a typical velocity of the membrane at some critical early time t^* when we believe instabilities are important. This critical time t^* likely falls in the range between the compressible time scale (10^{-6} s for our drops) and
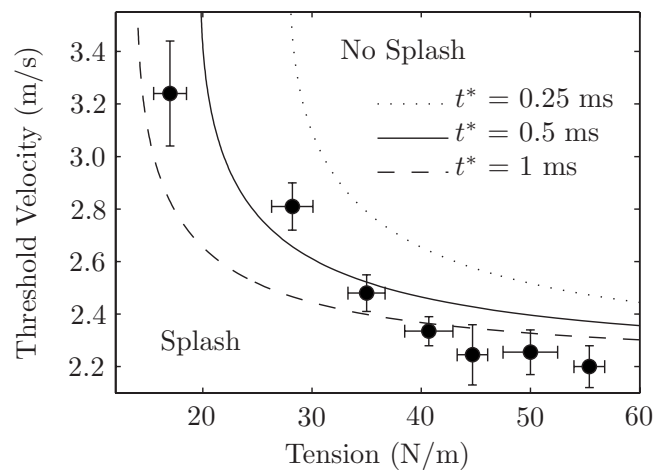

FIG. 8. Threshold velocity for splashing vs membrane tension for drops with $R_0 = 1.01 \pm 0.02$ mm, as in Fig. 3. The lines are calculated from Eq. (8) with $R_0 = 1.01$ mm, $V_{TS} = 2.2$ m/s, and t^* as listed in the figure.

the characteristic time scale for spreading ($2R_0/V_0 \approx 10^{-3}$ s for our drops). All the drop parameters (such as surface tension and viscosity) enter this equation through V_{TS}. Taking the derivative of δ [Eq. (7)] at t^* and substituting into $V_T - \dot{\delta}^* = V_{TS}$ yields

$$V_T - \frac{\rho R_0^{3/2} V_T^{5/2}}{T t^{*1/2}} = V_{TS}. \tag{8}$$

Equation (8) estimates the splash threshold V_T given R_0, T, and the measured V_{TS}, and its predictions are shown in Fig. 8 with a set of different values for t^*. Since many estimates have been made in our calculation of V_T, the times chosen in Fig. 8 represent the approximate order of magnitude of the time relevant for the splashing instability. The times shown ($t^* = 0.25 - 1$ ms) are therefore in rough accord with the time of maximum membrane deflection ($\simeq 0.4$ ms), at which we find a possible kinetic energy threshold, and with the time at which difference in lamella dynamics become insignificant ($\simeq 0.4$ ms). We find that Eq. (8) matches our data both in trend and order of magnitude, which is suggestive that our model captures much of the physics for the change in splashing threshold for liquid drop impact on a flexible membrane.

IV. CONCLUSION

We have examined an unexplored parameter to tune the splash of a liquid droplet on a solid substrate and studied its role in the splashing mechanism. By changing the compliance of the substrate, using variations in the tension in an elastic membrane, we show that splashing can be suppressed using a soft substrate. This approach is a novel way to reduce splashing in manufacturing processes and could also be important in pesticide delivery to leaves and other flexible surface. While the late-time energy balance is shown not to play a role in the splash, an early-time energy balance suggests a possible threshold criterion: the drop must retain a certain amount of kinetic energy after the membrane has fully

deformed in order to form a splash at later times. We also find indications that it is the very early times after impact that are critical for determining whether a splash occurs or not, as it is only at these times that the lamella dynamics are different for impacts on membranes of different tensions. Finally, we provide a model for the tension dependence of the threshold velocity for splashing using order-of-magnitude arguments for the impact pressure based on incompressible potential flow.

ACKNOWLEDGMENTS

[1] J. L. Zable, "Splatter during ink jet printing," IBM J. Res. Dev. **21**, 315 (1977).
[2] D. B. van Dam and C. Le Clerc, "Experimental study of the impact of an ink-jet printed droplet on a solid substrate," Phys. Fluids **16**, 3403 (2004).
[3] M. Gavaises, A. Theodorakakos, and G. Bergeles, "Modeling wall impaction of diesel sprays," Int. J. Heat Fluid Flow **17**, 130 (1996).
[4] S. Sampath and X. Jiang, "Splat formation and microstructure development during plasma spraying: Deposition temperature effects," Mater. Sci. Eng., A **304–306**, 144 (2001).
[5] W. Wirth, S. Storp, and W. Jacobsen, "Mechanisms controlling leaf retention of agricultural spray solutions," Pestic. Sci. **33**, 411 (1991).
[6] V. Bergeron, D. Bonn, J. Y. Martin, and L. Vovelle, "Controlling droplet deposition with polymer additives," Nature (London) **405**, 772 (2000).
[7] A. L. Yarin, "Drop impact dynamics: Splashing, spreading, receding, bouncing," Annu. Rev. Fluid Mech. **38**, 159 (2006).
[8] C. Mundo, M. Sommerfeld, and C. Tropea, "Droplet-wall collisions—Experimental studies of the deformation and breakup process," Int. J. Multiphase Flow **21**, 151 (1995).
[9] I. V. Roisman, K. Horvat, and C. Tropea, "Spray impact: Rim transverse instability initiating fingering and splash, and description of a secondary spray," Phys. Fluids **18**, 102104 (2006).
[10] A. L. Yarin and D. A. Weiss, "Impact of drops on solid-surfaces—Self-similar capillary waves, and splashing as a new-type of kinematic discontinuity," J. Fluid Mech. **283**, 141 (1995).
[11] C. Josserand and S. Zaleski, "Droplet splashing on a thin liquid film," Phys. Fluids **15**, 1650 (2003).
[12] L. Xu, W. W. Zhang, and S. R. Nagel, "Drop splashing on a dry smooth surface," Phys. Rev. Lett. **94**, 184505 (2005).
[13] J. Qian and C. K. Law, "Regimes of coalescense and seperation in droplet collision," J. Fluid Mech. **331**, 59 (1997).
[14] C. D. Stow and M. G. Hadfield, "An experimental investigation of fluid-flow resulting from the impact of a water drop with an unyielding dry surface," Proc. R. Soc. London, Ser. A **373**, 419 (1981).
[15] G. E. Cossali, A. Coghe, and M. Marengo, "The impact of a single drop on a wetted solid surface," Exp. Fluids **22**, 463 (1997).
[16] K. Range and F. Feuillebois, "Influence of surface roughness on liquid drop impact," J. Colloid Interface Sci. **203**, 16 (1998).
[17] L. Courbin, J. C. Bird, and H. A. Stone, "Splash and anti-splash: Observation and design," Chaos **16**, 041102 (2006).
[18] L. Xu, "Liquid drop splashing on smooth, rough, and textured surfaces," Phys. Rev. E **75**, 056316 (2007).
[19] C. Duez, C. Ybert, C. Clanet, and L. Bocquet, "Making a splash with water repellency," Nat. Phys. **3**, 180 (2007).
[20] J. E. Field, J. P. Dear, and J. E. Ogren, "The effects of target compliance on liquid-drop impact," J. Appl. Phys. **65**, 533 (1989).
[21] L. Courbin, A. Marchand, A. Vaziri, A. Ajdari, and H. A. Stone, "Impact dynamics for elastic membranes," Phys. Rev. Lett. **97**, 244301 (2006).
[22] S. Chandra and C. T. Avedisian, "On the collision of a droplet with a solid-surface," Proc. R. Soc. London, Ser. A **432**, 13 (1991).
[23] M. Pasandideh-Fard, Y. M. Qiao, S. Chandra, and J. Mostaghimi, "Capillary effects during droplet impact on a solid surface," Phys. Fluids **8**, 650 (1996).
[24] T. Mao, D. C. S. Kuhn, and H. Tran, "Spread and rebound of liquid droplets upon impact on flat surfaces," AIChE J. **43**, 2169 (1997).
[25] I. V. Roisman, R. Rioboo, and C. Tropea, "Normal impact of a liquid drop on a dry surface: Model for spreading and receding," Proc. R. Soc. London, Ser. A **458**, 1411 (2002).
[26] C. Ukiwe and D. Y. Kwok, "On the maximum spreading diameter of impacting droplets on well-prepared solid surfaces," Langmuir **21**, 666 (2005).
[27] P. Attane, F. Girard, and V. Morin, "An energy balance approach of the dynamics of drop impact on a solid surface," Phys. Fluids **19**, 012101 (2007).
[28] L. D. Landau and E. M. Lifshitz, *Theory of Elasticity* (Pergamon, New York, 1986).
[29] S. T. Thoroddsen and J. Sakakibara, "Evolution of the fingering pattern of an impacting drop." Phys. Fluids **10**, 1359 (1998). In particular, see p. 1369, col. 2, par. 2.
[30] H.-Y. Kim, Z. C. Feng, and J.-H. Chun, "Instability of a liquid jet emerging from a droplet upon collision with a solid surface," Phys. Fluids **12**, 531 (2000).
[31] R. F. Allen, "The role of surface tension in splashing," J. Colloid Interface Sci. **51**, 350 (1975).
[32] A. Antkowiak, N. Bremond, S. Le Dizes, and E. Villermaux, "Short-term dynamics of a density interface following an impact," J. Fluid Mech. **577**, 241 (2007).